Anal Bioanal Chem (2010) 397:2631–2646
DOI 10.1007/s00216-010-3700-1

REVIEW

Applications of Raman spectroscopy to gemology

Danilo Bersani · Pier Paolo Lottici

Received: 26 January 2010 / Revised: 26 March 2010 / Accepted: 29 March 2010 / Published online: 24 April 2010

Abstract Being nondestructive and requiring short measurement times, a low amount of material, and no sample preparation, Raman spectroscopy is used for routine investigation in the study of gemstone inclusions and treatments and for the characterization of mounted gems. In this work, a review of the use of laboratory Raman and micro-Raman spectrometers and of portable Raman systems in the gemology field is given, focusing on gem identification and on the evaluation of the composition, provenance, and genesis of gems. Many examples are shown of the use of Raman spectroscopy as a tool for the identification of imitations, synthetic gems, and enhancement treatments in natural gemstones. Some recent developments are described, with particular attention being given to the semiprecious stone jade and to two important organic materials used in jewelry, i.e., pearls and corals.

Keywords Raman spectroscopy · Gems · Minerals · Jade · Pearls · Corals

Introduction

Gemology is a complex field where many disciplines converge: natural sciences (geology, chemistry, physics, mineralogy, and crystallography), art, history, and archaeology. Economic aspects also play an important role in the study of gems.

D. Bersani (✉) · P. P. Lottici
Dipartimento di Fisica, Università di Parma,
Viale G.P. Usberti 7a,
43100 Parma, Italy
e-mail: danilo.bersani@fis.unipr.it

P. P. Lottici
e-mail: lottici@fis.unipr.it

One of the most important issues in gemological research is the classification of a gem, in terms of mineral species, purity, provenance, and identification of enhancement treatments. Obviously, it is of great importance that the analysis can be performed in a completely nondestructive and noninvasive way. In addition, the objects to be analyzed are in many cases macroscopic stones, often of great value, and sometimes they can be mounted on jewels, protected by glass, or enclosed in plastic containers.

Over 30 years ago few laboratories applied Raman spectroscopy to gemology [1–10]. Only in the last decade, with the availability of more compact and flexible instrumentation, have Raman and micro-Raman spectroscopy fully shown their possible applications in this field. In the past few years many gemological laboratories have been equipped with a Raman spectrometer, and the technique is now used for routine investigation for some specific aspects, such as gemstone inclusions and imitations, emerald and diamond treatments, and characterization of mounted gems [9].

Raman spectroscopy offers many advantages, such as short measurement times and the low amount of material required. For gemological purposes, it is particularly appreciated, being a completely noninvasive, contactless technique which does not require any sample preparation. Moreover, the use of portable apparatus allows the analysis of objects that cannot be moved, such as gems mounted on historic and archaeological artifacts preserved in a museum.

The economic value of a gem depends not only on its rarity, but also on its degree of purity, which is in turn related to lattice order and the absence of inclusions, and, in general, on its agreeable aspect. This last characteristic depends on the perfect planarity of the surfaces and on the color, often due to impurities. A good example is beryl, found in many colored varieties: green emerald due to Cr^{3+}

ions, blue aquamarine due to the simultaneous presence of Fe^{2+} and Fe^{3+}, pink morganite due to manganese, yellow heliodor due to Fe–O charge transfer, and the colorless goshenite. Defects can be responsible for the gem coloration, as in smoky quartz. Moreover, gemstones of the same variety may show considerable variations in cost owing to different shades or provenance. As an example, the pigeon's blood red shade of expensive Mogok rubies is due to the chromium ions, whereas other ions give rise to a lesser appreciated shade, such as the bluish tint given by iron and titanium to some Möng Hsu rubies [11, 12].

In addition, only few of the commercial gems are simply faceted gemstones, most being subjected to some enhancement treatment to obtain a more agreeable aspect, in terms of transparency and color. So, most of the stones are not completely "natural." To give a correct evaluation of a gem it is important to distinguish between untreated gems, gems that have received treatments which are considered acceptable by the gem market, and gems that have received heavy treatments, not acceptable by the market. Some heat treatments, not involving a phase transition, have been used for thousands of years [13] and are considered in some way traditional. As an example, most gem sellers accept as normal the heating of blue-green-shaded beryls to obtain blue aquamarine [14], whereas ion diffusion used to modify the color of a corundum is usually not acceptable and is considered as fraudulent [12, 14]. Stones with similar aspect have a great difference in value according to the kind of treatments; it is then very important to distinguish highly valued untreated gems from low-priced gems which have received heavy enhancements, and, obviously, to recognize synthetic stones (with the same composition as natural stones) or simulants (or imitations), which are natural or synthetic stones with a composition different from that of the simulated one. This aspect will be discussed in the following.

In the last 30–40 years, different papers have pointed out the main aspects of the applications of Raman spectroscopy to gemology [9, 10, 15–18]; in this work we would like to give a quick overview of the main topics, with a closer look at some recent developments.

Raman spectroscopy: the technique

The instrumentation for Raman spectroscopy may be divided into two families: laboratory systems, usually equipped with a microscope and multiple laser lines, and portable systems.

Portable systems are useful when gems are exhibited or held in public or private collections and cannot be transferred to the laboratory owing to their value or because they are mounted on large objects, or when they are unreachable, being displayed in a glass case [18]. Sometimes portable systems are the only possible choice; a fiber-optic head and large-working-distance objectives are very useful. Some of the most used fiber-optic probe heads, also used for applications in gemology, were described by Pitt et al. [19], together with a large overview of the Raman instrumentation. One of the main problems in the use of portable systems is the constant presence of mechanical vibrations, even when robust tripods are used. This often leads to the use of low-magnification objectives with a large working distance and low numerical aperture, causing a limitation in the collection of the scattered light. Usually portable systems are affected by the fluorescence of the material surrounding the point analyzed, more than laboratory systems, owing to their lack of confocality. The spectral resolution of true portable Raman spectrometers usually ranges between 4 and 10 cm^{-1} (much more than the 1–2 cm^{-1} of the standard laboratory systems), which is enough to identify most of the minerals, but not enough to perform compositional studies. Cheap ultraportable systems are also available on the market, but they have very low resolution and are often unable to work in the low-wavenumber part of the spectrum, in some cases being useless.

Overall, laboratory equipment offers better performance in terms of spectral and spatial resolution and acquisition times. Almost all modern Raman laboratory equipment has a micro-Raman configuration, being coupled with an optical microscope to focus the laser beam on the sample and collect the scattered light. The use of microscope objectives with magnification up to ×100 allows spatial resolution down to approximately 1 μm to be obtained. This fact, combined with the confocality of laboratory micro-Raman spectrometers, enables the analysis of fluid and solid inclusions in gemstones, minimizing the signal of the host matrix, and the detection of fissure filling. In addition, different excitation wavelengths can usually be chosen in laboratory systems: this is helpful to reduce the disturbing fluorescence, when present, and to improve the Raman signal when looking for resonance phenomena.

Even Fourier transform (FT)-based systems are effectively used in gemology. FT-Raman spectrometers are based on the same technology as widely used FT-IR instruments. They allow the use of long-wavelength excitation, usually produced by a Nd:YAG laser, at 1,064 nm, requiring a Michelson interferometer coupled with an IR detector, instead of a diffraction grating and a CCD as in standard dispersive systems. Low-energy excitation is very effective in reducing fluorescence, but in the study of gems such excitation is not as important as in other fields: the change of excitation in the visible range is often enough to limit the fluorescence effects. Fluorescence in gems and gemstones is often due to traces of rare

earth elements. In this case strong, sharp bands are obtained, which can be confused with the Raman signal [20]. When fluorescence of rare earth elements is present, FT-Raman spectroscopy cannot solve the problem either. FT-Raman spectroscopy has some disadvantages compared with dispersive systems, in particular a worse spatial resolution (5–10 vs. 1–2 μm for dispersive micro-Raman spectroscopy), lower sensitivity (2–3 orders of magnitude), and therefore the need for greater laser power and lower measurement speed [19].

There are some requirements to obtain good measurements: a polished surface normal to the laser beam usually gives a better Raman signal [10]; however, in such a configuration some plasma lines (secondary emissions of the laser) could be visible, disturbing the measurement in the low-wavenumber part of the spectrum.

Even when the laser spot is very small (it can be reduced down to 1-μm size), some additional peaks can be found owing to inclusions, dirt, fillers, and cutting or polishing materials (such as SiC, Cr_2O_3, Al_2O_3, SnO) [10]. It is therefore important to pay attention to the possible extra peaks, possibly by repeating the measurement at different points, to avoid mistakes.

One of the main issues is anisotropy of the crystals. In a single crystal, the relative intensities of the different Raman bands change dramatically according to the mutual orientation of the crystal axes and of the laser polarization. This orientational dependence is a powerful tool for crystallographic studies, but could cause mistakes when experimental results are compared with data in a database, as discussed in the following.

Raman spectroscopy can be fruitfully employed in teaching courses on gem identification owing to its ease of use [21].

Applications of Raman spectroscopy to gemology: identification

The first question to answer when looking at a gem is simply: what is it? The standard way to give an answer by means of Raman spectroscopy is by comparison of the spectral fingerprint of the gem with some spectra of standard minerals. Figure 1 shows the Raman spectra of some usual and unusual gems. Luckily, the availability of a large database of Raman spectra of mineral species is constantly increasing in time, so this question is often easy to answer using Raman spectroscopy. In particular, some databases are free on the Web [22–27], and even more extended databases with automatic search engines are commercially available. In the traditional literature, the situation is now not so different from the one described by Smith [18] a few years ago: some small catalogues of mineral species which could be relevant in gemology have been published [1, 28–35], but they often appear in Ph.D. theses which are difficult to access [32, 33], or are related to specific topics, such as corrosion products or pigments, or are in languages other than English [1].

The same answer is not so easy to obtain when dealing with rare gemstones whose Raman spectra are not reported in the databases, or when the correct identification is difficult owing to large similarities in the spectra of different species; the latter case is not so rare for minerals belonging to the same series with very similar composition and structure. It is obviously possible to extend the range of measurements, including some destructive techniques, to achieve a correct identification, but this may not be a routine method with rare and highly valuable gems. Thus, it is very important that papers allowing the correct identification of a rare gemstone through its Raman spectrum are published. As an example, Kiefert et al. [9] showed how to distinguish between rare the Be–Al–Mg oxides taaffeite and musgravite.

The comparison between the Raman spectrum obtained on a gem and a standard one could be complicated by the different relative orientations between the crystallographic axis of the mineral and the polarization axis of the excitation laser, and to some extent by the dependence of the spectrometer's sensitivity on the polarization of the scattered light. Raman polarizability is a nine-element tensor relating, for each vibrational mode, the amplitudes of the *x*, *y*, and *z* components of the electric field in the light scattered by the Raman effect to the components of the electric field of the incident light [36, 37]. Even in the case of an ideal spectrometer, with a response independent of the

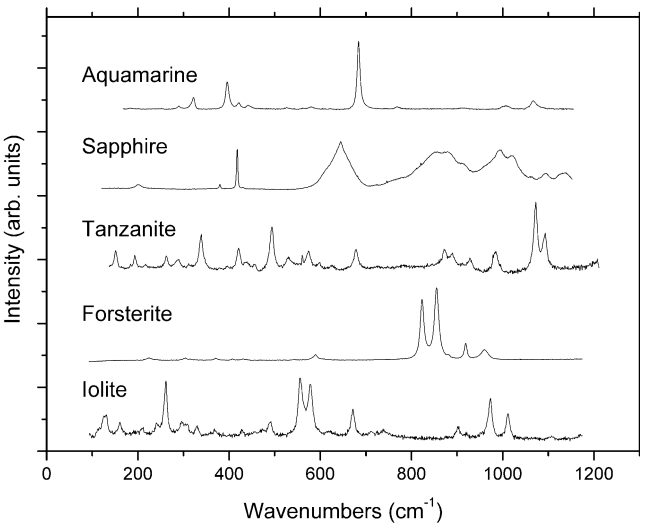

Fig. 1 Raman spectra, obtained with 632.8-nm excitation, of some usual (aquamarine and sapphire) and unusual (tanzanite, forsterite, and iolite, a variety of cordierite) gems. In the spectrum of sapphire, all the features at wavenumbers higher than 600 cm^{-1} are due to fluorescence

polarization of the light, the intensity of each Raman peak would depend on the relative orientation between the laser polarization and the crystal axes. In most cases the gems are obtained from single-crystal gemstones and the shape and orientation of the cut gems depend on the crystalline system, the symmetry, the crystal habit, and cleavage. The main edges of the gems are therefore often related in a simple way to the crystallographic axis, and it is common to obtain Raman spectra in which one or more peaks are absent, owing to a particular orientation. Raman spectra obtained in two perpendicular configurations in nonmonometric species may be very different. This could be misleading when the spectra are compared with spectra in a database, in particular when an automatic search in electronic databases is used. However, this fact is actually helpful to obtain information on the symmetry and orientation of a gem, and in particular to determine if it is a single crystal, a polycrystal, or a geminate. Figure 2 shows as examples the spectra obtained in two orthogonal orientations on topaz [$Al_2SiO_4(F,OH)_2$] and on the unusual gem danburite [$CaB_2(SiO_4)_2$]. The changes in the relative intensities of the Raman features are clearly visible, whereas their wavenumbers are almost the same. The apparent shift of the 930–940-cm^{-1} band of topaz is due to the presence of two partly overlapping peaks, at 927 and 938 cm^{-1}, visible in different geometries.

The resonance effects must also be taken into account when trying to identify a gem using Raman spectroscopy. Resonance occurs when either the excitation or the scattered light has energy equal to or very close to a real electronic transition of the material analyzed. This leads to a large increase in the whole Raman signal and is often accompanied by a change in the relative intensities of the different peaks. The latter aspect could add some difficulty when the spectrum acquired on a gem is compared with spectra reported in a database obtained with a different laser line because the overall aspect of the spectrum could be different, even if the wavenumbers of the peaks are the same. However, the enhancement due to resonance can sometimes be useful to obtain fast and clear identification of materials which usually give a weak signal.

Many gems are well-defined mineral species, such as diamond (C); most gemstones are silicates, such as beryl, topaz [$Al_2SiO_4(F,OH)_2$], and zircon ($ZrSiO_4$), whereas the second most represented class is oxides, such as ruby and sapphire (Al_2O_3) [18]. In this case the mineralogical species of a gem is quite easy to identify, by means of comparison with literature spectra. As previously stated, even though no comprehensive gemstone Raman database has been built yet, an increasing number of papers with gem spectra has been published in the last 30 years [1–3, 28–35, 38, 39]. Huang [8] provided spectra of some gems, and reported an interesting flowchart useful to discriminate between the most common gems starting from the main Raman peaks.

Varieties of the same species are often present, even with different colors and aspects, but belonging to the same species. Emerald and aquamarine have different colors, and often different commercial value too, but both are beryl ($Al_2Be_3Si_6O_{18}$). This means that their chemical composition is almost the same, differing only for impurities (Fe^{2+} and Fe^{3+} in aquamarine, Cr and V in emerald), which are responsible for the color [40–42]. Usually these small variations cannot produce visible effects in the Raman spectra, but major variations in chemistry may be reflected in small intensity and frequency changes in the peaks. Moroz et al. [43] showed how these changes could be useful to distinguish emeralds of different provenance.

As for many other spectroscopies, multivariate techniques are being increasingly used for the analysis of Raman spectra. Del Castillo et al. [11] showed how an automatic system can be implemented for the quick verification of the nature of a large number of semiprecious stones. For multivariate analysis, the database should contain spectra from many samples of the same mineral measured in different conditions, to take into account small chemical variations and different experimental conditions. The method presented [11] uses the spectra of the RRUFF database [22] and is able to quickly collect spectra of 96 samples mounted on a multiwell plate.

Applications of Raman spectroscopy to gemology: composition

In many cases, gems belong to a mineral group which constitutes an isomorphic series whose chemical composition changes continuously within a specified range. The extreme terms of the compositional range are the so-called end members of the series and, in general, every member of the group can be considered a solid-state solution of the end members. Tourmalines and garnets are examples of gems which do not correspond to mineral species but to mineral groups. Knowledge of the actual composition of a gem, which could be expressed as the percentage of the various end members of the group, is important to give a correct estimation of its value and provenance.

One of the most important examples of the use of Raman spectroscopy in determining the composition of gems is that of garnets. Minerals belonging to the garnet group have the general formula $A_3^{2+}B_2^{3+}(SiO_4)_3$ (A is Ca, Fe^{2+}, Mn^{2+}, Mg; B is Al, Cr^{3+}, Fe^{3+}). This isomorph group is usually divided into two series: pyralspites (pyrope $Mg_3Al_2Si_3O_{12}$, almandine $Fe_3Al_2Si_3O_{12}$, spessartine $Mn_3Al_2Si_3O_{12}$) and ugrandites (uvarovite $Ca_3Cr_2Si_3O_{12}$, grossular $Ca_3Al_2Si_3O_{12}$, andradite $Ca_3Fe_2Si_3O_{12}$) [44, 45]. Gemstones corresponding

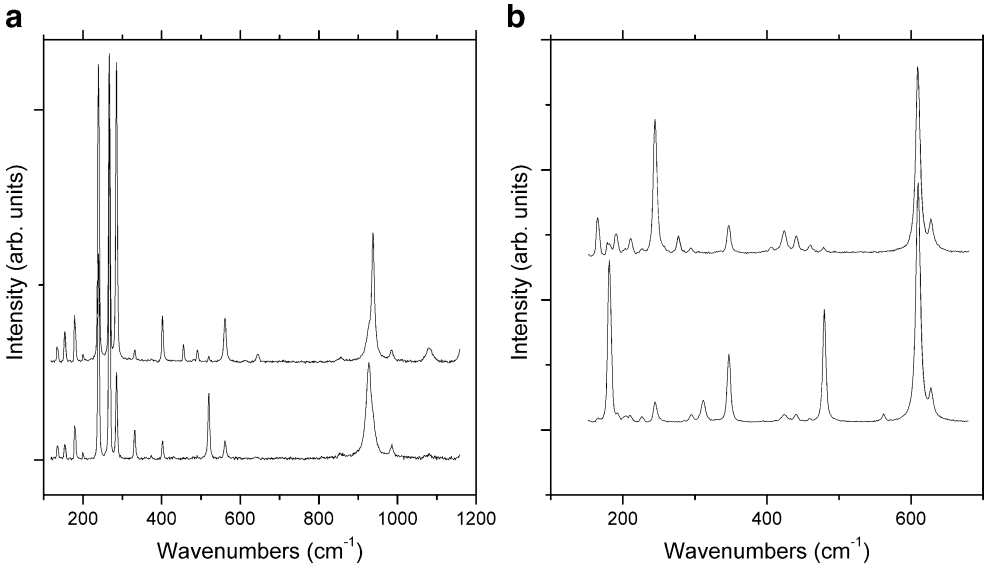

Fig. 2 Raman spectra of **a** topaz [$Al_2SiO_4(F,OH)_2$] and **b** danburite [$CaB_2(SiO_4)_2$]. The spectra were obtained for two orthogonal orientations of the samples

to pure end members are rare in nature, so the composition of a generic garnet crystal could be described as Alm_{xAlm}·Spe_{xSpe}·Pyr_{xPyr}·Gro_{xGro}·And_{xAnd}·Uva_{xUva} (Alm is almandine, Spe is spessartine, Pyr is pyrope, Gro is grossular, And is andradite, Uva is uvarovite). As in most series, not all the composition occurs in nature, but a miscibility gap exists between pyralspites and ugrandites [46, 47]. The possibility to obtain the composition of a garnet crystal starting from its Raman spectrum was presented and largely discussed by Smith and coworkers [48–51], including application to gemology [51] and, recently, by Ando et al. [52–54]. The proposed methods are based on the fact that for most of the Raman bands in the spectra of garnet solid solutions, an almost one-mode behavior is expected [48–51, 55]. This means that the frequency of a Raman peak may be obtained by means of a linear combination of the frequencies of the end members weighted by their molar ratio: $\nu = x_{\mathrm{Alm}}\nu_{\mathrm{Alm}} + x_{\mathrm{Spe}}\nu_{\mathrm{Spe}} + x_{\mathrm{Pyr}}\nu_{\mathrm{Pyr}} + x_{\mathrm{Gro}}\nu_{\mathrm{Gro}} + x_{\mathrm{And}}\nu_{\mathrm{And}} + x_{\mathrm{Uva}}\nu_{\mathrm{Uva}}$.

The Raman spectra of garnets [55–60] in the ugrandite and pyralspite series are shown in Fig. 3. The method presented by Bersani et al. [53], called micro-Raman garnets evaluation method (MIRAGEM), uses minimization software, working in a MATLAB® environment (version R2007B), and calculates the composition (x_{Alm}, x_{Spe}, x_{Pyr}, x_{Gro}, x_{And}, x_{Uva}) that better reproduces the frequencies measured in the Raman spectrum of the sample. As an example, Fig. 4 shows a comparison between the andradite contents in garnets of the andradite—grossular series measured by wavelength-dispersive spectrometry–electron microprobe analysis and calculated by MIRAGEM: a good agreement is found, with differences lower than 5%.

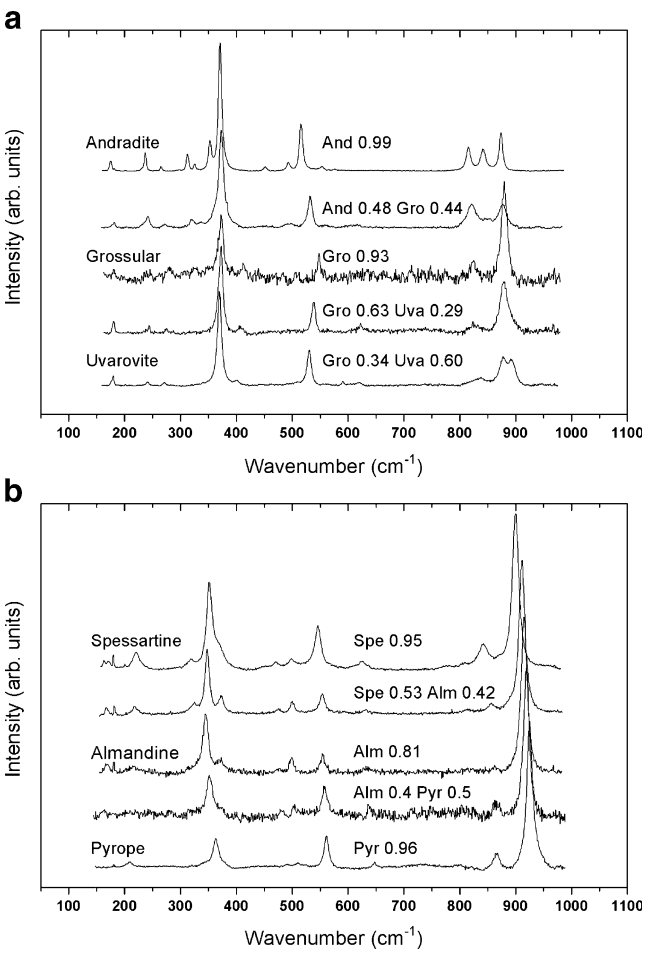

Fig. 3 Raman spectra of garnets in the ugrandite (**a**) and pyralspite (**b**) series. (Reprinted with permission from Bersani et al. [54], copyright 2009, American Institute of Physics)

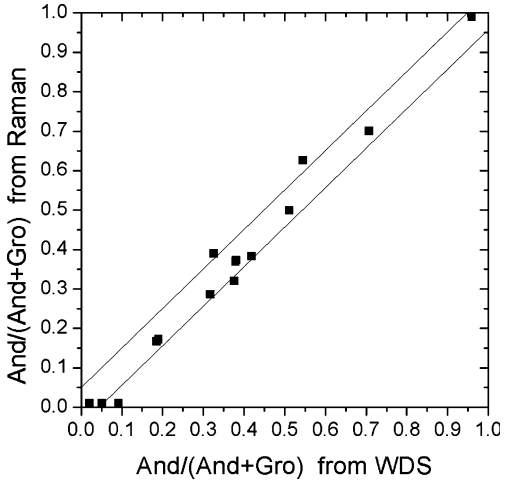

Fig. 4 Comparison between the andradite contents in garnets of the andradite–grossular series measured by wavelength-dispersive spectrometry (*WDS*)–electron microprobe analysis and calculated by Raman spectroscopy. The ±5% lines are drawn for visual aid. (Reprinted with permission from Bersani et al. [54], copyright 2009, American Institute of Physics)

The proposed method could be extended to other mineral groups of interest for gemology, after adequate calibration of the method based on an accurate measurement of the frequencies for a large number of compositions. However, this method only works when the vibrational modes have one-mode behavior, and this means that only isomorph series are suitable.

Many other examples of identification of gems and gemstone species are present in the literature. Kuebler et al. [61] used Raman spectra to obtain the composition of olivine, which is usually a solid solution of the end members forsterite and fayalite. The frequencies of both peaks of the strong doublet that occurs in the spectral region of 815–825 and 838–857 cm^{-1} show monotonic shifts following cation substitution between forsterite and fayalite. This allows one to obtain the forsterite contents in terms of the Mg/(Mg + Fe) molar ratio. In this work, not only was an estimation of the chemical composition obtained from Raman spectra, but also information on crystal structure (distinction of polymorphs).

Other groups of interest in gemology have been characterized in terms of correlation between Raman spectra and compositions in works developed outside the field of gemology. A wide study to obtain the composition of different pyroxenes was reported in [62]; the minerals analyzed were not gems and the paper dealt with planetary science, however the results could be applied to identification of stones sometimes used in jewelry, such as jadeite, diopside, and spodumene.

A further example shows how Raman spectroscopy may provide some subtle information, beyond simple composition [63]. Nephrite is a variety of tremolite–actinolite of the amphibole group, used in jewelry as a green semiprecious stone. In addition to the identification of materials, the variable iron and magnesium contents were investigated. The fine structure of the OH stretching vibration band of the Raman spectra of nephrite depends on the electronegativity of the bonded cations. The study of this fine structure allows estimation of the cation distribution in nephrite, which is responsible for the coloration, and is associated with different geological conditions and so can help in provenance studies.

Even the quality of some gems, in terms of long-range order and the presence of impurities, can be assessed by Raman spectroscopy. As an example, the width and the position of the sharp peak at 1,332.7 cm^{-1} may be used to evaluate lattice order in diamonds [64]. On the other hand, a broad band is observed at 1,500 cm^{-1} for an impure sample [64]. Raman spectrometers are also often used for photoluminescence measurements in diamonds and emeralds, to evaluate their quality, detect nitrogen impurities, and study the bleaching mechanism [43, 65, 66].

Applications of Raman spectroscopy to gemology: provenance and genesis

The investigation of the origin of gems by means of Raman spectroscopy could be done in two ways. The first one is the study of slight variations in the vibrational spectra related to small differences in composition or to the presence of some extra elements typical of some localities or geological environments [43, 67].

A very interesting example is given from the combined inductively coupled plasma, IR, Raman, and NMR study of some beryls from the Sudety mountains [67], where it was shown how Raman spectroscopy can create a new classification scheme for beryl. The classification takes into account the content of alkalis in the beryl structure and is based on the ratio between two types of water molecules, whose stretching modes are measured at 3,609–3,606 cm^{-1} (not connected with alkali) and at 3,597–3,594 cm^{-1} (hydrated anions of alkali). Beryl may be classified in three groups: alkali-free, alkali-poor, and alkali-rich beryls. In addition, polarized Raman measurements in the spectral region characteristic of the CO_2 Fermi doublet (1,386–1,240 cm^{-1}) show the orientation (perpendicular to the *c*-axis) of CO_2 molecules in the structural channels of beryl.

The second and most practiced way to obtain information on provenance and genesis of gems and gemstones by Raman spectroscopy is the study of solid or fluid inclusions. Inclusions in gemstones are receiving great

interest because they are a sort of ID of the gemstone, containing a large amount of information on its origin [68–70]. Inclusions embedded in the host crystals can be studied by using a confocal micro-Raman spectrometer which enables detection of materials below the external surface of the gem. Decreasing the diameter of the confocal hole in the spectrometer will reduce the region of collection of the Raman signal, down to a few micrometers in *x*, *y*, and *z* directions. This allows optimization of the Raman signal of the inclusion analyzed and minimizes the contribution from the host matrix. Figure 5 shows the Raman spectra obtained on a needle-shaped inclusion in a garnet gem. The Raman spectrum of the host garnet allows its identification as a pyrope–almandine type, whereas the spectrum of the inclusion, after the subtraction of the matrix signal, is characteristic of rutile.

Raman spectroscopy is therefore largely used in the identification of inclusions in minerals and gems [10, 71–89]. In the following, some examples, in particular on corundum, are reported together with some particular applications.

Corundum

Corundum (Al_2O_3; ruby and sapphire) is probably the most important example of the use of inclusions for provenance and genesis studies; many works are present in the literature, sometimes with useful tables correlating mineralogical species present such as inclusions, with geological settings and localities [72, 90–95].

Delé et al. [90] provided a list of the most common solid inclusions in ruby from some classic localities. The distinction is possible because some mineral inclusions are characteristic of different parageneses: pyroxene and nepheline occur in volcanic veins (Thailand, Cambodia), calcite, amphibole, and spinel occur in metamorphic carbonates (Myanmar), whereas quartz and apatite occur in metasomatic seams (Vietnam). Palanza et al. [91] identified a variety of inclusions observed in sapphires, not only as a function of the geological origin but, in some cases, of specific deposits. Although some minerals, such as rutile, are not specific, being present in both magmatic and metamorphic sapphires, other minerals are characteristic of the geological origin: zircon inclusions surrounded by dark halos are typical of alkali basalt, and diaspore, calcite, and CO_2 are typical of marbles.

Fluid inclusions are used to study provenance of corundum gemstones. Updated tables of inclusions and a wide bibliography, and good examples of the use of Raman spectroscopy on fluid and solid inclusions combined with many different techniques for the elaboration of detailed genetic models of corundum deposits (i.e., trace element analyses by inductively coupled plasma mass spectroscopy, optical absorption spectrometry, colorimetry, electron microprobe, and isotopic analyses) are given in [94, 95].

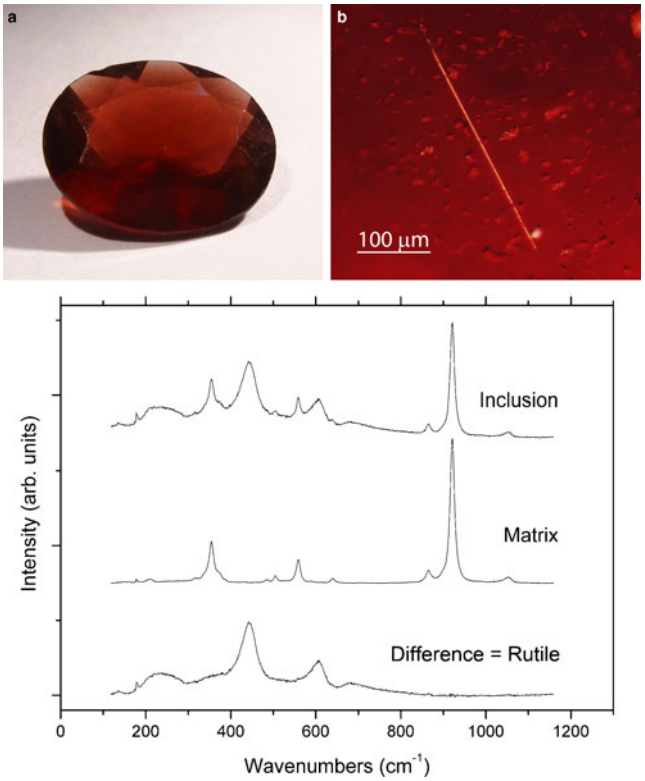

Fig. 5 A pyrope–almandine garnet (**a**), a needle-shaped inclusion (**b**) and their Raman spectra. The difference spectrum, characteristic of rutile, is reported

Modern Raman instrumentation equipped with motorized scanning tables allows one to obtain two- and three-dimensional spectral maps of crystals and their inclusions. A huge amount of information is then available for the analysis of inclusions using statistical methods. An example was reported by Sutherland et al. [93], where the occurrence of different types of inclusions in rubies (anatase, rutile, CO_2, sulfured compounds, apatite, and zircon) was evaluated with the aim to distinguish between two Vietnamese mines.

The laser-induced fluorescence in the visible range sometimes appears in the form of sharp and well-defined bands, in particular when rare earth elements are present as impurities in the crystal lattice. In these cases, fluorescence could be used to detect rare earth elements in gemstones such as corundum and zircon, suggesting a hypothesis for their provenance, genesis, and age [93, 96, 97]. The wavelength of the fluorescence lines depends not only on the specific element, but also on the local crystal field around the ion and then on the host mineral. The apparent Raman shift of a fluorescence line, as well as its intensity, obviously depends on the wavelength of the excitation laser line. As an example, Eu^{3+} and Er^{3+} in zircon produce lines

in the range 543–558 nm, appearing in the Raman spectra as peaks between 1,010 and 1,500 cm^{-1} excitation is at 514.5 nm [96].

Diamonds and other gems

Inclusions in diamonds can be used to determine the provenance of gems or identify the original host rocks when the gemstones are found in large alluvial deposits [73, 98, 99].

Raman spectroscopy is used to identify mineral species in sealed inclusions in diamonds and to estimate their remnant pressure. Inclusions such as garnet, clinopyroxene, titanite, melilite, and anatase have been identified. These results, combined with a diamond inclusion model [100], allow one to estimate temperature and pressure ranges of diamond formations, and suggest hypotheses for the diamond's age and storage conditions.

Residual pressure is a key point to reconstruct the thermobarometric history of a diamond crystal. Accurate measurement of the wavenumbers of the main Raman peaks of both diamond (at nearly 1,332 cm^{-1}) and inclusions [101], whose position is pressure-dependant, is a very sensitive tool to evaluate pressure.

Recent developments, allowed by the use of fast spectrometers equipped with motorized stages, give three-dimensional Raman maps in diamond crystals around mineral inclusions. The spectral maps can be converted into detailed pressure maps by means of Gaussian fitting procedures and of models correlating peak position with pressure [102]. The method proposed by Kagi et al. [102] simultaneously yields pressure and temperature conditions at which mineral inclusions were trapped in the diamond, using Raman data only.

Dating of gems and gemstones is an important tool to identify their provenance, understand the formation mechanisms, and possibly locate new deposits. In this particular field, micro-Raman spectroscopy may help for a better interpretation of the results of dating techniques. As an example, we report a recent study on apatite, a calcium phosphate sometimes used as a gem and often present as inclusion in many gemstones. In the fission-track thermochronometry of apatites, the dating starts when the crystal temperature falls below a characteristic threshold temperature; at higher temperatures the fission tracks produced by uranium impurities in the crystal are annealed and disappear. The threshold temperature depends on the chemistry and cell parameters of each apatite crystal. Zattin et al. [103] suggested Raman spectroscopy as a routine tool to calibrate apatite crystallographic structure to correct dating results; in particular, a strong correlation between cell parameter *a* and the variation of Raman shift in the 452–440-cm^{-1} range was shown.

Applications of Raman spectroscopy to gemology: imitations, synthetic gems, and enhancement treatments

As previously stated, one of the most important challenges in gemology is the identification of enhancement treatments in natural gemstones [104, 105]. Overviews of the most employed techniques to enhance different gems, such as heating, fissure filling, ion diffusion, radiation exposure, coating, bleaching, dyeing, and impregnation, are given in [14, 16, 106].

The filling of fissures in gems with oils and other substances to enhance their clarity is a common practice, in particular in emeralds. Many substances are used for this purpose: oils, waxes, Canada balsams, and epoxy resins such as Opticon, Palma, and Permasafe [16]. The organic fillers can be identified by comparison with reference spectra, in the spectral "fingerprint" region of the organic compounds, between 1,200 and 1,800 cm^{-1}, where C–O and C–C stretching modes are visible and where inorganic crystals usually show very few and weak peaks, or no peaks at all. The characterization of the filler is important because some substances (such as oils) are accepted in the trade as fillers, being unable to polymerize, whereas other substances, such as epoxy resins, are not accepted because after polymerization their removal is very difficult [16].

Not only organic materials are used to fill fissures: some highly fractured rubies are filled with high-refractive-index glass to improve their clarity [107]. Recently, glass fillers have been identified in rubies using Raman spectroscopy: Fan et al. [108] recognized the use of lead glass (broad and strong Raman band close to 1,563 cm^{-1}) combined with an organic substance in the cracks.

Corundum, as ruby and sapphire, is one of the gemstones most subject to a variety of enhancement treatments owing to the large number of low-quality crystals available on the market. In addition to fissure fillings, heating is one of the most used gem treatments, usually accepted among jewelers; it is often assumed that all corundum gemstones have been heated to some extent. Many other enhancement treatments are not considered as acceptable, owing to irreversible modifications [11]. This is the case of "flux healing," obtained by partial surface melting to hide fractures; the melting is achieved using flux agents such as borax, calcium borate ($Ca_2B_2O_6{\cdot}5H_2O$), and calcium or sodium phosphate [$Ca_3(PO_4)_2$, Na_3PO_4]. Micro-Raman spectroscopy could be used to find traces of flux agents on the corundum surface [11].

A particular corundum treatment has been gaining in use in the past few years, i.e., beryllium color diffusion, used to obtain pink–orange corundum or cancel purplish cores in rubies [11, 12, 109]. Heating the corundum together with chrysoberyl ($BeAl_2O_4$) causes the diffusion of beryllium. Be^{2+} ions trap holes, yielding yellow to orange coloration.

Sastry et al. [109] recently proved that Raman spectroscopy is able to detect the structural disorder induced by beryllium diffusion treatment in rubies and sapphires. The valence changes produced by beryllium diffusion and the possible dissolution of natural inclusions disturb the long-range order of the corundum lattice, leading to an overall broadening of the Raman spectra and to the disappearance of some vibrational modes. This can help to detect treated stones.

The detection of imitations is often an easy task using Raman spectroscopy, owing to different compositions compared with the real gems, as is the case with cubic zirconia used as an imitation of diamond [21] and other stones [110]. Figure 6 shows the Raman spectra of diamond, of its most common simulant cubic zirconium oxide, and of another imitation, strontium titanate.

More puzzling is the recognition of synthetic gems with the same composition and structure as the natural ones. A good overview of gemstone synthesis techniques is reported in [111]. One of the main tools to recognize synthetic gems is the identification of solid and fluid inclusions [39, 112, 113]. As an example, Delé et al. [90] identified the synthetic corundum produced by the flux method by looking for the presence in gems of inclusions of flux, such as cryolite, tungstates, and polymolybdates.

Applications of Raman spectroscopy to gemology: historical and archaeological gems

Minerals are present in almost every field of conservation science: they are found in many objects with archaeological, historical or artistic interest, in the form of pigments, lapidary materials, corrosion products, ceramics, and so on.

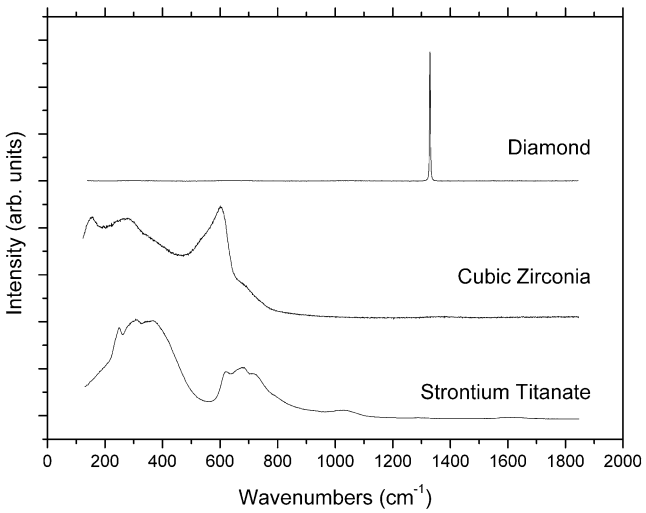

Fig. 6 Raman spectra of diamond and of its simulants, cubic zirconium oxide and strontium titanate

Raman spectroscopy is well suited for nondestructive studies of mineral species in the fields of art and archaeology and, in particular, of gems and gemstones used for art objects [9, 15, 17, 28, 29, 35, 114–119]. Many cases involving archaeological gems, including the spotting of a doublet, were reported by Smith and Clark [15]. Gemstones on art items of the Basel Cathedral Treasury (Reliquary Cross, Dorothy Monstrance, and Head Reliquary of St. Eustace) have been studied by means of both portable and fixed Raman systems [120, 121]. The adorning gemstones on the reliquary Heinrich's Cross from the treasury of Basel Cathedral, kept in the Museum of Applied Arts (Kunstgewerbemuseum), Berlin, were investigated by Reiche et al. [122].

Raman spectrometry was used to identify most of the mineral inclusions (apatite, zircon, ilmenite, monazite, calcite, quartz) present in almandine garnets in Merovingian jewelry [71]. Several gemstones in the cover of the Tours Gospel, "Evangelia Quatuor," held in the British Library were identified by means of Raman microscopy by Clark and van der Weerd [123]. The large collection of minerals and rocks of the Prussian kings in the Grotto Hall of the New Palace, Park Sanssouci in Potsdam, was identified by means of a mobile Raman microprobe [124].

Even stones *in sensu latu*, such as glass gemstones in archaeological rings, should be studied with Raman spectroscopy, allowing one to collect technological information on the glass production (fictive temperature, raw materials) [125, 126].

Applications of Raman spectroscopy to gemology: semiprecious stones, jade

Raman spectroscopy is largely used for the study of semiprecious minerals and stones too. Raman spectroscopy has proven to be very effective in the identification of types of opal (amorphous or CT) [127, 128]. Details on the Raman study of jade are reported in the following.

This gem, "royal gem" in China, was used in prehistoric times as an ideal tough material for weapons and tools, and is known in many fine nuances of green, but also in shades of white, black, gray, yellow, and orange, and in delicate violet tones. The term "jade" refers to two minerals, nephrite (an amphibole) and jadeite (a pyroxene) [129]: nephrite was used in China until the eighteenth century, when jadeite was imported from Burma. Jadeite and nephrite are both regarded in China as "genuine jade."

Nephrite belongs to the tremolite–ferroactinolite [$Ca_2Mg_5Si_8O_{22}(OH)_2$, $Ca_2Fe_5Si_8O_{22}(OH)_2$] series. Jadeite corresponds to the mineral species with composition $NaAlSi_2O_6$: it is one of the end members of the clinopyroxene group, where chemical substitutions of Na (in the M2

site), Al (in the M1 site), or Si (in the tetrahedral site) are possible [18].

Fine-quality jadeite is the rarer and more commercially valuable of the two gems. The distinction between nephrite and jadeite is particularly important. On the other hand, a variety of less-valued other minerals or artificial materials were used as "true jade," and identification is important in the assessment of authenticity. Raman microscopy allowed the identification of materials used for antique Chinese jade artifacts [130–133].

An investigation on jade artifacts from the British Museum and standard geological samples [134] enabled the composition of nephrite to be estimated by analyzing the OH vibrations in the Raman spectra which were found to occur in the range 3,671–3,623 cm^{-1}, according to the Fe/(Fe+Mg) ratio [134]. The use of Raman spectroscopy to determine Fe/(Fe+Mg) ratios (% pfu) in jades has proven itself to be a useful method of classifying artifacts and gaining insight into their geological origins [135]. As previously discussed, a correlation between color and cation distribution in six nephrite jade artifacts dated from the Neolithic period to the Han dynasty (about 3000 BC to 220 AD) was obtained through the study of the fine structure of the OH stretching Raman vibration band [63].

The Si–O–Si symmetric stretching vibration of jadeite is affected by the nature of the M2 cation and, to a lesser extent, by the M1 cation [18]: the wavenumber of the corresponding spectral band (in the 650–750-cm^{-1} range) may give indirect "chemical" information on the actual composition, after suitable calibration [18].

Raman spectra of jadeite jade from Mesoamerica, on both artifacts and rocks, have been extensively investigated [18, 136–140]. The jadeite or nephrite nature of jade Chinese artifacts from the Trésor of the Muséum National d'Histoire Naturelle in Paris was determined by means of Raman spectroscopy [141, 142]: distinguishing features are the Si–O–Si stretching vibration at 675 cm^{-1} (nephrite) and above 695 cm^{-1} (jadeite), and the presence of OH stretching vibrations for nephrite.

Not only good and natural jade is offered for sale, often fake or poor-quality products or stones which have been colored or otherwise treated are too. Raman spectroscopy has been widely reported, especially in Chinese scientific literature, for the identification of various jadeite jade and other jades [143, 144].

Jadeite (and albite) of violet color (probably due to Mn^{3+} ions replacing Al^{3+}) was reported by Hänni et al. [77]. Raman spectroscopy has been used to detect graphite inclusions in nephrite jade [145]. A dark-green jade, called "inky jadeite jade," is found to consist of over 85–90% pyroxene omphacite [146].

Raman studies have been reported on yellow serpentine jade [147], pink jadeite jade with white ribbons [148], zoisite jade "red-green jewelry" [149], illite jade ("Zipao jade") [150], and idocrase jade (vesuvianite, californite, American jade) [151]. A "fake" Dushan jade from Nanyang, Henan province, has been investigated [152] by means of Raman and other techniques: the major mineral components in Dushan jade are plagioclase (mostly anorthite) and zeolite. Antigorite is found in Xiuyan jade [153].

Structural and vibrational (Raman and FT-IR) comparisons between jadeite and synthetic jadeite show that the two species are hardly distinguishable [154]. Some jade in the marketplace has been dyed, chemically bleached, coated with paraffin, wax or some resin, and/or impregnated by a polymer. Other known treatments, used singly, together, or along with those just mentioned, include the application of acid (commonly acetic acid) or a bleach to remove extraneous stains or other coatings, and heating to improve colors. A Raman spectroscopy study of heat-treated nephrite up to 800 °C was carried out to investigate if heat treatments were used to facilitate jade carving or modify the color of jade in ancient China, or if it was burned during a funeral ceremony, or even if heat treatment can give the appearance of naturally weathered jades [155].

The "bleaching" treatment of jadeite jade is a two-step process whereby a brown or gray component (probably iron compounds) is removed chemically, followed by impregnation of the resulting white to green material with some type of polymer. The treatment product is commonly referred to as "bleached jadeite" or "B jade" in the Orient. Raman spectroscopy has been found to be a useful tool for identification of bleached and polymer-impregnated jadeites. The major advantage over classic methods of gem testing is the nondestructive identification of inclusions in gemstones and the determination of organic fracture filling in jade. Micro-Raman spectroscopy has been used [108] to investigate bleached and filled jadeite jade: bleaching with strong acid produces microcracks, which are filled with epoxy resin, evidenced by the Raman shifts close to 777, 1,123, 1,611, 2,930, and 3,065 cm^{-1}. Moreover, it is possible to identify bleached jade by distinguishing resin from paraffin [156].

Applications of Raman spectroscopy to gemology: organic materials (pearls, corals)

Pearls

Pearls are organic gems, created when an oyster covers a foreign object with layers of "mother of pearl," or nacre. Nowadays, pearls are cultured in different mollusks in both seawater (Akoya and South) and freshwater.

A pearl is composed of 93–95% calcium carbonate ($CaCO_3$) (in all three polymorphic modifications calcite,

aragonite, and vaterite), 5% organic matrix (including hard proteins, β-chitin, and polysaccharides), and 1% moisture. The outer part of a pearl is composed of alternating sheets of aragonite and organic matrix.

In pearl analysis, Raman spectroscopy [9, 10] has focused on the polymorphism of biogenic carbonate with the corresponding vibrational band assignment [157–159], or has been used to differentiate between natural and artificially colored cultured pearls [16, 21, 160].

Vaterite (μ-$CaCO_3$) and aragonite polymorphs in freshwater-cultured pearls have been mapped and characterized by means of Raman spectroscopy [161–164] (for both Japanese and Chinese beaded and nonbeaded freshwater-cultured pearls), and the role of vaterite in the biomineralization process has been discussed. A complete study of the Raman spectroscopy of synthetic, geological, and biological vaterite was presented by the same authors [165].

The orientation of the biogenic aragonite mineral growth in pearls has been investigated by means of polarized micro-Raman scattering [166]: the pearl surface layers correlate to the *ab* crystallographic plane of aragonite, and the radial direction to the *c*-axis of an aragonite crystal. This is shown in Fig. 7, where the Raman spectra obtained on an aragonite crystal, with the laser polarization parallel and perpendicular to the *c*-axis, and on the surface of a pearl, with random orientation, are compared. The similarities between the spectra of pearl and aragonite in the *ab*-plane (perpendicular to the *c*-axis) are evident, as well as the differences between the pearl spectrum and the aragonite spectrum along the c-axis.

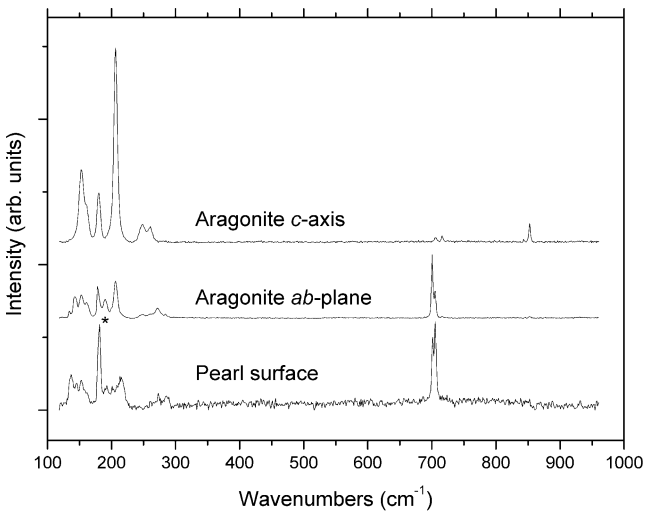

Fig. 7 Raman spectra obtained on an aragonite crystal, with the laser polarization parallel to the *c*-axis and to *ab*-plane, and on the surface of a pearl. The spectra are normalized on the strong 1,087-cm^{-1} peak (not shown). *Asterisk* plasma line

Dumanska-Slowik et al. [167] claimed that discrimination between spontaneously nucleated natural pearls and freshwater-cultured tissue-graft Chinese pearls is possible owing to the absence of Raman peaks at 1,133 and 1,526 cm^{-1} which are supposed to be typical of natural pearls. This conclusion was criticized by Karampelas [168].

Nacre is the internal lustrous "mother of pearl" layer of many molluskan shells, composed of flat polygonal crystals of aragonite and organic compounds in-between. The biomineralization process for the nacre formation [169] and the in vitro growth of aragonite crystal on the nacre surface [170] have been investigated by means of Raman microscopy.

The nature of pigments in naturally colored pearls is still under discussion (as in the case of corals). Raman evidence of metalloporphyrins in nacre of shells of Peteria penguin was reported in [171]. In freshwater-cultured pearls the nature and distribution of pigments responsible for different coloration (in both nacre and pearl) have been extensively studied using micro-Raman spectroscopy, with several excitation wavelengths [162, 171, 172]. The frequency positions of the C–C single bond stretching vibration and C=C double bond stretching vibration are used to identify the chain length of specific polyenes or carotenoids. The exact position of the C=C stretching vibration of polyenic molecules depends strongly on the number of double bonds contained in the polyenic chain [172–175].

Soldati et al. [162] identified ten different pigments in vaterite; the color is attributed to the combination of unmethylated polyenes with chain lengths between eight and 12 conjugated double bonds. Methylated and unmethylated polyene pigments with no limitation on the chain length were found in aragonite. According to Barnaard and de Waal [176], the pigments found in molluskan biogenic matrix are polyenes, with unmethylated polyacetylenic backbones of various conjugation lengths. The role of polyenes in the coloration of freshwater-cultured pearls was further investigated by Karampelas et al. [174]; they proposed mixed unmethylated (unsubstituted) polyenes, not carotenoids, for natural-color *Hyriopsis* samples. The same result was found for Chinese freshwater pearls of different colors [177] (with three different excitation wavelengths and compared with carotenoid pigments found in eggshells). Polyenes were also detected by means of resonance Raman microspectrometry, such as molluskan shell pigments [178].

Two important pearl-culturing mollusk shells, *Pinctada martensii* and *Hyriopsis cuningii*, have been studied [179]: aragonite and carotenoids were found in nacreous and prismatic layers in *Hyriopsis cumingii*, whereas shells of *Pinctada martensii* show calcite.

The discrimination between freshwater- and seawater-cultured pearls may be made by means of X-ray fluores-

cence: the manganese content is higher in freshwater pearls, whereas the strontium content is higher in seawater-cultured pearls [180]. Raman analysis of the $CaCO_3$ major vibrations using statistical methods was proposed to discriminate between freshwater pearls and seawater pearls (Akoya and South) by Park et al. [181].

Tahitian pearls (natural black), irradiated freshwater-cultured pearls, black-dyed freshwater-cultured pearls, and irradiated and dyed pearls are also characterized by means of Raman spectroscopy: only Tahitian pearls show porphyrin peaks in the Raman spectra [182]. Freshwater pearls dyed black with a silver nitrate solution [183] show Raman spectra with a distinct peak at 570 cm^{-1}, corresponding to some Ag–O vibrations of silver oxide on the pearl's surface, whereas a peak at 240 cm^{-1} could be ascribed to silver nitrate [10].

A difference in the intensity of a peak at 275 cm^{-1} in the Raman spectrum has been found between golden saltwater and color-treated pearls, owing to the larger fluorescence background in the latter case [184], and this could be used to discriminate between them. Some information on golden seawater-cultured pearls and golden-dyed pearls was obtained by Raman spectroscopy [185, 186]. Chocolate pearls have been investigated by means of Raman spectra [187]. The relatively rare phenomenon of iridescence on the outer surface of seashells was investigated by means of Raman spectroscopy by Brink and van der Berg [188], revealing a mixture of porous aragonite and organic materials such as carotenoids, which would change the overall refractive index.

Corals

Like pearls, corals are organic jewelry materials too. Apart from black and gold corals, formed by hornlike organic matter [189], corals consist of over 90% calcium carbonate in aragonite or calcite forms. The formation and nature of calcium carbonate have obviously been deeply investigated by means of Raman spectroscopy [157, 190–195]. Raman spectra of biogenic carbonates from corals, both pink pigmented and unpigmented, mainly show bands which are typical of aragonite. In soft corals (*Porites* sp.) the features are slightly broader than the corresponding bands for natural pearls, and this is ascribed to some positional disordering of carbonate ions resulting from some (less than 10%) substitution of magnesium for calcium ions[157] in calcite.

Micro-Raman spectroscopy was employed to study black corals [196]. Unlike the skeletons of their red and white relatives, the skeleton of black corals is mainly composed of organic matter (chitin fibrils admixed with peptides): Nowak et al. [196] reported a Raman mapping of the fibrils.

The nature of the dyes responsible for the natural color in pink-to-red corals has been largely investigated by means of Raman spectroscopy [197–200], and the scientific debate on their nature continues [176, 189, 191, 198, 199, 201–203]. Carotenoids or mixtures of polyenes (unsubstituted, unmethylated, polyenes) [175, 189, 204] have been proposed. The polyenic nature of the dyes responsible for the color of corals has been determined at different excitation wavelengths, by studying the characteristic C=C stretching vibrations, whose frequencies seem to depend on the polyenic chain length, and the C–C stretching vibrations, whose frequencies are more influenced by the presence of the $–CH_3$ substituting groups in carotenoids [173, 175, 201, 202]. Canthaxanthin (a β-carotene derivative) has been found in *Corallium rubrum*, the most famous red coral [205].

Raman scattering may be helpful to distinguish between endangered and more commercial coral species [201] through the identification of their calcite or aragonite structure, or differences in the pigments (carotenoids or unmethylated polyenic pigments).

The supply of high-quality pink-to-red natural-color coral has dramatically decreased in recent years, whereas the quantity of "artificially" dyed coral has increased. Raman analysis can establish conclusively if the color is natural or obtained by dyeing, by the presence of the characteristic carotene or unmethylated polyene peaks (the most intense at about 1,520 and 1,120 cm^{-1}) [190].

Conclusions

Raman spectroscopy means speed, sensitivity, micrometric resolution, and nondestructive testing, and meets the requirements of gemology. With a standard micro-Raman apparatus, equipped with two or three lasers in different parts of the visible (and near-IR) range, it is possible to obtain information on the nature of the gems, their composition, structure, and purity, to identify inclusions and to detect enhancement treatments. Recent developments have shown the use of Raman spectroscopy to obtain quantitative information on the composition of gemstones.

Raman analysis is not limited to inorganic crystals, being able to obtain information also on organic gemological materials (corals, ambers, and pearls), or amorphous or nanocrystalline materials (obsidian, opal). The use of a portable spectrometer expands the range of investigations, allowing the analysis of gems preserved in museums or mounted on archaeological or historical artworks.

Raman spectroscopy can be used as a standard tool in gemological laboratories and it use should develop among gem sellers for quick identification. Raman measurements are fast and inexpensive (except for the purchase of the

spectrometer), and could be routinely done not only on top-valued gems but also on semiprecious stones.

Raman spectroscopy shows its applications especially in the field of gemological research, providing important contributions to the study of the genesis and provenance of gems. The analysis of slight modifications of the vibrational spectrum and the accurate study of micrometric fluid and solid inclusions can reveal important details on the geological history of the minerals.

In perspective, the diffusion of fast systems to obtain two- and three-dimensional spectral maps, the use of multivariate techniques to analyze large amounts of data, and the production of integrated instrumentation where use of Raman spectrometers is coupled with different techniques (such as scanning electron microscopy–energy dispersive X-ray spectroscopy or FT-IR spectroscopy) will further extend the applications of Raman spectroscopy in gemological research. On the other hand, the diffusion of comprehensive databases of Raman spectra of minerals, the automation of routine measurements of large numbers of samples, and the possibility to obtain fast identification of the gems and their composition with an adequate degree of confidence, using user-friendly software and hardware systems, will help the diffusion of this technique outside research laboratories.

References

1. Pinet M, Smith DC, Lasnier B (1992) In: La microsonde Raman en gemmologie. Schubnel H-J, Smith DC (eds) Revue de gemmologie A F G, No. special hors série. Association Francaise de Gemmologie, Paris, Chapt. II, pp 11–61
2. Hanni HA, Kiefert L, Chalain J-P, Wilcock I (1997) J Gemm 25:394–406
3. Dhamelincourt P, Schubnel H-J (1977) Rev Fr Gemmol 52:11–14
4. Delé-Dubois M-L, Dhamelincourt P, Schubnel H-J (1981) Rev Fr Gemmol 63:13–14
5. Delé-Dubois M-L, Dhamelincourt P, Schubnel H-J (1981) Rev Fr Gemmol 64:13–16
6. Lasnier B (1995) Anal Mag 23:16–18
7. Schubnel H-J (1992) In: La microsonde Raman en gemmologie. Schubnel H-J, Smith DC (eds) Revue de gemmologie A F G, No. special hors série, Association Francaise de Gemmologie, Paris, Chapt. II, pp 5–10
8. Huang E (1999) J Geol Soc China 42:301–318
9. Kiefert L, Chalain JP, Haberli S (2005) In: Edwards HGM, Chalmers JM (eds) Raman Spectroscopy in archaeology and art history. RSC analytical spectroscopy monographs. Royal Society of Chemistry, Cambridge, pp 379–402
10. Kiefert L, Hanni HA, Ostertag T (2001) In: Lewis IR, Edwards HGM (eds) Handbook of Raman spectroscopy: from the research laboratory to the process line. Marcel Dekker, New York, pp 469–490
11. del Castillo HC, Deprez N, Dupuis T, Mathis F, Deneckere A, Vandenabeele P, Calderon T, Strivay D (2009) Anal Bioanal Chem 394:1043–1058
12. Emmett JL, Scarratt K, McClure SF, Moses T, Douthit TR, Hughes R, Novak S, Shigley JE, Wang WY, Bordelon O, Kane RE (2003) Gems Gemol 39:84–135
13. Overton TW, Shigley JE (2008) Gems Gemol 44:32–55
14. Shigley JE (2008) Geologija 50:227–236
15. Smith GD, Clark RJH (2004) J Archaeol Sci 31:1137–1160
16. Kiefert L, Hanni HA, Chalain JP (2000) Proc SPIE 4098:241–251
17. Vandenabeele P, Edwards HGM, Moens L (2007) Chem Rev 107:675–686
18. Smith DC (2005) In: Edwards HGM, Chalmers JM (eds) Raman spectroscopy in archaeology and art history. RSC analytical spectroscopy monographs. Royal Society of Chemistry, Cambridge, pp 335–378
19. Pitt GD, Batchelder DN, Bennett R, Bormett RW, Hayward IP, Smith BJE, Williams KPJ, Yang YY, Baldwin KJ, Webster S (2005) IEE Proc Sci Meas Technol 152:241–318
20. Makreski P, Jovanovski G (2008) J Raman Spectrosc 39:1210–1213
21. Aponick A, Marchozzi E, Johnston C, Wigal CT (1998) J Chem Educ 75:465–466
22. RRUFF Project (2010) Department of Geosciences, University of Arizona, Tucson, USA. http://rruff.info/. Accessed 10 Mar 2010
23. Minerals Raman Database (2010) Physics Department, University of Parma, Italy. http://www.fis.unipr.it/phevix/ramandb.html. Accessed 10 Mar 2010
24. Romanian Database of Raman Spectroscopy (2010) Department of Geology, The Alexandru Ioan Cuza University, Iasi, Romania. http://rdrs.uaic.ro/. Accessed 10 Mar 2010
25. Handbook of Minerals Raman Spectra (2010) Ecole normale supérieure de Lyon, Lyon. http://www.ens-lyon.fr/LST/Raman/index.php. Accessed 10 Mar 2010
26. RASMIN, Raman Spectra Database of Minerals and Inorganic Materials (2010) National Institute of Advanced Industrial Science and Technology (AIST), Japan. http://riodb.ibase.aist.go.jp/rasmin/. Accessed 10 Mar 2010
27. Raman spectra database, Dipartimento di Scienze della Terra, Università di Siena (2010). http://www.dst.unisi.it/geofluids/raman/spectrum_frame.htm. Accessed 10 Mar 2010
28. Bouchard M, Smith DC (2005) In: Edwards HGM, Chalmers JM (eds) Raman spectroscopy in archaeology and art history. RSC analytical spectroscopy monographs. Royal Society of Chemistry, Cambridge, pp 429–464
29. Bouchard M, Smith DC (2003) Spectrochim Acta A 59:2247–2266
30. Smith DC, Boyer H, Pinet M (1987) International Conference GEORAMAN '86, Ecole Normale, Paris, France, Abstracts Volume, Terra Cognita 7, 20
31. Bény C, Lasnier B, Malézieux J (1989) International Conference GEORAMAN '89: Contributions, Special. Pub., ANRT, Association National de la Recherche Technique, Paris, p 2
32. Maestrati R (1989) Contribution à l'édification du catalogue Raman des gemmes, Diploma DUG memoir, Nantes University, France
33. Bouchard M (2001) Évaluation des Capacités de la Microscopie Raman dans la Caractérisation Minéralogique et Physico-chimique de Matériaux Archéologiques : Métaux, Vitraux & Pigments, Thèse de Doctorat, Muséum National d'Histoire Naturelle, Paris
34. Bell IM, Clark RJH, Gibbs PJ (1997) Spectrochim Acta A 53:2159–2179
35. Burgio L, Clark RJH (2001) Spectrochim Acta A 57:1491–1521
36. Long DA (1977) Raman spectroscopy. McGraw-Hill, New York
37. Nakamoto K (2009) Infrared and Raman spectra of inorganic and coordination compounds: theory and applications in inorganic chemistry. Wiley-Interscience, Hoboken1

38. Delé-Dubois M-L, Poirot JP, Schubnel H-J (1986) Rev Gemmol 88:15
39. Delé-Dubois M-L, Dhamelincourt P, Poirot JP, Schubnel H-J (1986) J Mol Struct 143:135
40. Spinolo G, Fontana I, Galli A (2007) Phys Status Solidi B 244:4660–4668
41. Parkin KM, Loeffler BM, Burns RG (1977) Phys Chem Miner 1:301–311
42. Nassau K (1978) Am Mineral 63:219–229
43. Moroz I, Roth M, Boudeulle M, Panczer G (2000) J Raman Spectrosc 31:485–490
44. Novak GA, Gibbs GV (1971) Am Mineral 56:791–825
45. Deer WA, Howie RA, Zussman J (1982) Rock-forming minerals. Orthosilicates, Halsted
46. Berman RG (1990) Am Mineral 75:328–344
47. Ganguly J, Cheng W, Tirone M (1996) Contrib Mineral Petrol 126:137–151
48. Pinet M, Smith DC (1994) Schweiz Mineral Petrogr Mitt 74:161–179
49. Pinet M, Smith DC (1993) Schweiz Mineral Petrogr Mitt 73:21–40
50. Smith DC (2005) Spectrochim Acta A 61:2299–2314
51. Smith DC (2002) Acta Univ Carol Geol 46:87–89
52. Ando S, Bersani D, Vignola P, Garzanti E (2009) Spectrochim Acta A 73:450–455
53. Bersani D, Andò S, Vignola P, Moltiflori G, Marino I-G, Lottici PP, Diella V (2009) Spectrochim Acta A 73:484–491
54. Bersani D, Andò S, Vignola P, Moltifiori G, Marino I-G, Lottici PP, Diella V (2009) Spectrochim Acta A 73:484–491
55. Chopelas A (2005) Phys Chem Miner 32:525–530
56. Hofmeister AM, Chopelas A (1991) Am Mineral 76:880–891
57. Hofmeister AM, Chopelas A (1991) Phys Chem Miner 17:503–526
58. Geiger CA (2008) Am Mineral 93:360–372
59. Kolesov BA, Geiger CA (1998) Phys Chem Miner 25:142–151
60. Kolesov BA, Geiger CA (1997) J Raman Spectrosc 28:659–662
61. Kuebler KE, Jolliff BL, Wang A, Haskin LA (2006) Geochim Cosmochim Acta 70:6201–6222
62. Wang A, Jolliff BL, Haskin LA, Kuebler KE, Viskupic KM (2001) Am Mineral 86:790–806
63. Chen TH, Calligaro T, Pages-Camagna S, Menu M (2004) Appl Phys A Mater 79:177–180
64. Choudhary D, Bellare J (2000) Ceram Int 26:73–85
65. Dejanin B, Simic D, Zaitsev A, Chapman J, Dobrinets I, Widemann A, Del Re N, Middleton T, Dejanin E, De Stefano A (2008) Diamond Relat Mater 17:1169–1178
66. Collins AT, Kanda H, Kitawaki H (2000) Diamond Relat Mater 9:113–122
67. Lodzinski M, Sitarz M, Stec K, Kozanecki M, Fojud Z, Jurga S (2005) J Mol Struct 744:1005–1015
68. Gubelin EJ, Koivula JI (2008) Photoatlas of inclusions in gemstones, vol 3. Opinio, Basel
69. Gubelin EJ, Koivula JI (2005) Photoatlas of inclusions in gemstones, vol 2. Opinio, Basel
70. Gubelin EJ, Koivula JI (1986) Photoatlas of inclusions in gemstones, vol 1. Opinio, Basel
71. Calligaro T, Colinart S, Poirot JP, Sudres C (2002) Nucl Instrum Methods B 189:320–327
72. Dao NQ, Delaigue L (2000) Analusis 28:34–38
73. Smith CB, Bulanova GP, Kohn SC, Milledge HJ, Hall AE, Griffin BJ, Pearson DG (2009) Lithos 112(Suppl 2):822–832
74. Sodo A, Nardone M, Ajò D, Pozza G, Bicchieri M (2003) J Cult Herit 4:317s–320s
75. Schmetzer K, Hanni H, Bernhardt H-J, Schwarz D (1996) Gems Gemol 32:242
76. Krzemnicki MS (1999) Gems Gemol 35:192–195
77. Hanni H, Kiefert L, Chalain JP (1997) J Gemmol 25:394
78. Naumov VB, Kamenetsky VS, Thomas R, Kononkova NN, Ryzhenko BN (2008) Geochem Int 46:554–564
79. Bersani D, Salvioli-Mariani E, Mattioli M, Menichetti M, Lottici PP (2009) Spectrochim Acta A 73:443–449
80. Salvioli-Mariani E, Toscani L, Bersani D (2004) Mineral Mag 68:83–100
81. Sachanbinski T, Weber-Weller A, Sobczak T (2003) Pol Tow Mineral 22:189–192
82. Łodziński M, Michalik M (2004) Pol Tow Mineral 24:271–274
83. Vapnik Y, Moroz I (2002) Mineral Mag 66:201–213
84. Schwarz D (1994) Gems Gemol 30:88–101
85. Moroz I, Vapnik Y, Eliezri I, Roth M (2001) J Afr Earth Sci 33:377–390
86. Graham IT, Zaw K, Cook NJ (2008) Ore Geol Rev 34:1–2
87. Park GS, Bae SC, Granick S, Lee JH, Bae SD, Kim T, Zuo JM (2007) Diamond Relat Mater 16:397–400
88. Limtrakun P, Zaw K, Ryan CG, Mernagh TP (2001) Mineral Mag 65:725–735
89. Krzemnicki M (1999) Gems Gemol 35:192–195
90. Delé ML, Dhamelincourt P, Poirot JP, Dereppe JM, Moreaux C (1997) J Raman Spectrosc 28:673–676
91. Palanza V, Di Martino D, Paleari A, Spinolo G, Prosperi L (2008) J Raman Spectrosc 39:1007–1011
92. Sachanbinski M, Girulski R, Ulanski J, Kozaneck M (2003) Pol Tow Mineral 22:185–188
93. Sutherland FL, Duroc-Danner JM, Meffre S (2008) Ore Geol Rev 34:155–168
94. Graham I, Sutherland L, Zaw K, Nechaev V, Khanchuk A (2008) Ore Geol Rev 34:200–215
95. Garnier V, Giuliani G, Ohnenstetter D, Fallick AE, Dubessy J, Banks D, Vinh HQ, Lhomme T, Maluski H, Pecher A, Bakhsh KA, Van Long P, Trinh PT, Schwarz D (2008) Ore Geol Rev 34:169–191
96. Wopenka B, Jolliff BL, Zinner E, Kremser DT (1996) Am Mineral 81:902–912
97. Beloussova EA, Walters S, Griffin WL, O' Reilly SY, Fisher NI (2002) Contrib Mineral Petrol 143:602–622
98. Barron LM, Barron BJ, Mernagh TP, Birch WD (2008) Ore Geol Rev 34:76–86
99. Barron LM, Mernagh TP, Pogson R, Barron BJ (2008) 9th International Kimberlite Conference, Frankfurt, Germany, Extended Abstract No. 9IKC-A-00039
100. Barron LM (2005) Can Mineral 43:203–224
101. Izraeli ES, Harris JW, Navon O (1999) Earth Planet Sci Lett 173:351–360
102. Kagi H, Odake S, Fukura S, Zedgenizov DA (2009) Russ Geol Geophys 50:1183–1187
103. Zattin M, Bersani D, Carter A (2007) Chem Geol 240:197–204
104. McClure SF, Smith CP (2000) Gems Gemol 36:336–359
105. Sarma N (1993) Endeavour 17:7–11
106. Smith C, McClure S (2002) Gems Gemol 38:294–300
107. McClure S, Smith C, Wang W, Hall M (2006) Gems Gemol 42:22–36
108. Fan J-L, Guo S-G, Liu X-L (2009) Spectrosc Lett 42:129–135
109. Sastry MD, Mane SN, Gaonkar MP, Bagla H, Panjikar J, Ramachandran KT (2009) IOP Conf Ser Mater Sci Eng 2:012007
110. Kiefert L, Krzemnicki MS, Du Toit G, Befi R, Schmetzer K (2006) Proceedings of the Fourth International Gemological Symposium and GIA Gemological Research Conference. Gems Gemol 42:113–114
111. Oishi S (2003) In: Byrappa K, Ohachi T (eds) Crystal growth technology. William Andrew-Springer, New York, pp 561–580
112. Shigley J, McClure S, Cole J, Koivula J, Lu T, Elen S, Demianets L (2001) Gems Gemol 37:42–55

113. Schmetzer K, Kiefert L, Bernhardt H-J (1999) J Gemmol 26:487
114. Edwards HGM, Chalmers JM (eds) (2005) Raman spectroscopy in archaeology and art history. RSC analytical spectroscopy monographs. Royal Society of Chemistry, Cambridge
115. Bersani D, Lottici PP, Casoli A (2005) In: Edwards HGM, Chalmers JM (eds) Raman spectroscopy in archaeology and art history. RSC analytical spectroscopy monographs. Royal Society of Chemistry, Cambridge, pp 130–141
116. Smith DC (2006) In: Maggetti M, Messiga B (eds) Geomaterials in cultural heritage. Geological Society special publication, vol 257. Geological Society, London, pp 9–32
117. Bersani D, Antonioli G, Lottici PP, Casoli A (2003) Spectrochim Acta A 59:2409–2417
118. Bersani D, Campani E, Casoli A, Lottici R, Marina IG (2008) Anal Chim Acta 610:74–79
119. Ospitali F, Bersani D, Di Lonardo G, Lottici PP (2008) J Raman Spectrosc 39:1066–1073
120. Hänni HA, Schubiger B, Kiefert L, Haberli S (1998) Gems Gemol 34:102
121. Joyner L, Freestone I, Robinson J (2006) J Gemmol 30:169–182
122. Reiche I, Pages-Camagna S, Lambacher L (2004) J Raman Spectrosc 35:719–725
123. Clark RJH, van der Weerd J (2004) J Raman Spectrosc 35:279–283
124. Ziemann MA (2006) J Raman Spectrosc 37:1019–1025
125. Cesaratto A, Sichel P, Bersani D, Lottici PP, Montenero A, Salvioli-Mariani E, Catarsi M (2010) J Raman Spectrosc. doi:10.1002/jrs.2613
126. Colomban P (2003) J Non-Cryst Solids 323:180–187
127. Gaillou E, Delaunay A, Rondeau B, Bouhnik-Le-Coz M, Fritsch E, Cornen G, Monnier C (2008) Ore Geol Rev 34:113–126
128. Ostrooumov M, Fritsch E, Lasnier B, Lefrant S (1999) Eur J Mineral 11:899–908
129. Middleton A, Freestone I (1995) In: Rawson J (ed) Chinese jade. British Museum Press, London, p 413
130. Lien C-M, Tan L-P, Yu B-S (1996) Acta Geol Taiwan 32:121–129
131. Xu J-A, Huang E, Chen CH, Tan LP, Yu B-S (1996) Acta Geol Taiwan 32:11
132. Shurvell HF, Rintoul L, Fredericks PM (2001) Int J Vib Spectrosc 5:Sect 2
133. Liou Y-S (2003) West Pac Earth Sci 3:69
134. Middleton A, Ambers J (2005) In: Edwards HGM, Chalmers JM (eds) Raman spectroscopy in archaeology and art history. RSC analytical spectroscopy monographs. Royal Society of Chemistry, Cambridge, pp 403–411
135. Casadio F, Douglas JG, Faber KT (2007) Anal Bioanal Chem 387:791–801
136. Smith DC, Gendron F (1997) Abstr Suppl No 1 Terra Nova 9:35
137. Smith DC, Gendron F (1997) J Raman Spectrosc 28:731–738
138. Smith DC, Gendron F, Gautier F (1996) Terra Abst Suppl 2 Terra Nova 3
139. Gendron F, Smith DC, Gendron-Badou A (2002) J Archaeol Sci 29:837–851
140. Gendron F, Gendron-Badou A (1999) Rev Gemmol 16:36
141. Rondeau B, Smith DC (2000) ANRT Commission 48: spectrométries Raman: Innovation et Perspectives, Paris
142. Smith DC (2001) Colloquium: Raman spectroscopy in archaeology and art history. British Museum, London
143. Zhao H-X, Gan F-X (2009) Guangpuxue Yu Guangpu Fenxi 29:2989–2993
144. Zhang B, Gao Y, Ou Y (2001) Baoshi He Baoshixue Zazhi 3:22–26
145. Gu X, Qiu Z, Li Y, Yang P, Li L (2007) Zhongshan Daxue Xuebao Ziran Kexueban 46:141–142
146. Mei OYC, Qi LJ, Li H, Kwok B (2003) J Gemmol 28:337
147. Xue L, Wang Y-Q, Fan J-L (2009) Jiguang Yu Hongwai 39:267–270
148. Ouyang Q, Li H, Guo X, Yan J (2006) Baoshi He Baoshixue Zazhi 8:1–3
149. Chen Y-L, Zhong H (2007) Yankuang Ceshi 26:465–468
150. Zhou Y, Zhou R, Cao S, He Q (2006) Baoshi He Baoshixue Zazhi 8:10–12
151. Yu X, Ke J, Lei Y (2005) Baoshi He Baoshixue Zazhi 7:14–17
152. Liu Z, Gan F, Cheng H, Guo J (2008) Guisuanyan Xuebao 36:1330–1334
153. Liu Z, Gan F, Cheng H, Guo J (2009) Yanshi Xuebao 25:1281–1287
154. Cao S-M, Qi L-J, Guo Q-H, Zhong Z-Q, Qiu Z-L, Li Z-G (2008) Guangpuxue Yu Guangpu Fenxi 28:847–851
155. Chen TH (2008) Phase Transit 81:205–216
156. Zu E-D, Chen D-P, Zhang P-X (2003) Guang Pu Xue Yu Guang Pu Fen Xi 23:64–66
157. Urmos J, Sharma SK, Mackenzie FT (1991) Am Mineral 76:641–646
158. Rousseau M, Lopez E, Coute A, Mascarel G, Smith DC, Naslain R, Bourrat X (2005) J Struct Biol 149:149–157
159. Huang F, Yun X, Yang M, Chen Z (2003) J Gemmol 28:449–462
160. Li L, Chen Z (2001) J Gemmol 27
161. Jacob DE, Soldati AL, Wehrmeister U (2007) Geochim Cosmochim Acta 71:A434–A434
162. Soldati AL, Jacob DE, Wehrmeister U, Hager T, Hofmeister W (2008) J Raman Spectrosc 39:525–536
163. Soldati AL, Jacob DF, Wehrmeister J, Hofmeister W (2008) Mineral Mag 72:579–592
164. Wehrmeister U, Jacob DE, Soldati AL, Haeger T, Hofmeister W (2007) J Gemmol 31:399
165. Wehrmeister U, Soldati AL, Jacob DE, Häger T, Hofmeister W (2009) J Raman Spectrosc 41:193–201
166. Lu R (2009) GIA laboratory report. GIA, New York
167. Dumanska-Slowik M, Heflik W, Natkaniec-Nowak L, Sikorska M, Weselucha-Birczynska A (2008) Aust Gemmol 23:290–299
168. Karampelas S (2009) Aust Gemmol 23:473–474
169. Rousseau M, Lopez E, Coute A, Mascarel G, Smith DC, Naslain R, Bourrat X (2004) Key Eng Mater 254–256:1009–1012
170. Luo C, Xie L, Wang X-X (2007) Key Eng Mater 330–332:1335–1338
171. Zhang G, Xie X, Wang Y (2001) Guangpuxue Yu Guangpu Fenxi 21:193–196
172. Karampelas S, Fritsch E, Mevellec JY, Gauthier JP, Sklavounos S, Soldatos T (2007) J Raman Spectrosc 38:217–230
173. Schaffer HE, Chance RR, Silbey RJ, Knoll K, Schrock RR (1991) J Chem Phys 94:4161–4170
174. Karampelas S, Fritsch E, Mevellec JY, Sklavounos S, Soldatos T (2009) Eur J Mineral 21:85–97
175. Fritsch E, Karampelas S (2008) Spectrochim Acta A 71:1627–1627
176. Barnard W, de Waal D (2006) J Raman Spectrosc 37:342–352
177. Qin Z-L, Ma H-Y, Mu S-C, Tong Z-F (2007) Kuangwu Xuebao 27:73–76
178. Hedegaard C, Bardeau J-F, Chateigner D (2006) J Molluscan Stud 72:157
179. Zhang G-S, Xie X-D (2003) Fenxi Kexue Xuebao 19:27–29
180. Li L-P (2009) Diqiu Kexue 34:752–758
181. Park SC, Kim M, Park J, Chung H, Kim HY (2009) J Raman Spectrosc 40:2187–2192
182. Li G, Yu X, Cai K (2006) Guilin Gongxueyuan Xuebao 26:184–186
183. Thongnopkun P, Ekgasit S (2008) KMITL Sci J 8
184. Chen Y, Guo S, Shi L (2009) Guangxue Xuebao 29:1706–1709

185. Qi L, Huang Y, Zeng C (2008) Baoshi He Baoshixue Zazhi 10:1–8
186. Liu W-W, Li L-P (2007) Baoshi He Baoshixue Zazhi 9:33–36
187. Qi L, Huang Y, Zeng C (2008) Baoshi He Baoshixue Zazhi 10:20–24
188. Brink DJ, van der Berg NG (2005) J Phys D Appl Phys 38:338–343
189. Kupka T, Lin HM, Stobinacuteski L, Chen C-H, Liou W-J, Wrzalik R, Flisak Z (2010) J Raman Spectrosc (in press)
190. Smith C, McClure S, Eaton-Magaña S, Kondo D (2007) Gems Gemol 43:4–15
191. Kaczorowska B, Hacura A, Kupka T, Wrzalik R, Talik E, Pasterny G, Matuszewska A (2003) Anal Bioanal Chem 377:1032–1037
192. Zakaria FZ, Mihaly J, Sajo I, Katona R, Hajba L, Aziz FA, Mink J (2008) J Raman Spectrosc 39:1204–1209
193. Rahman MA, Oomori T (2008) J Cryst Growth 310:3528–3534
194. Gao Y, Zhang H (2002) Baoshi He Baoshixue Zazhi 4:20–23
195. Perrin C, Smith DC (2007) J Sediment Res 77:495–507
196. Nowak D, Florek M, Nowak J, Kwiatek W, Lekki J, Chevallier P, Hacura A, Wrzalik R, Ben-Nissan B, Van Grieken R, Kuczumow A (2009) Mater Sci Eng C Biomim Supramol Syst 29:1029–1038
197. Delé-Dubois ML, Merlin JC (1981) Hoseki Gakkaishi 8:161–168
198. Merlin JC, Delé ML (1983) Bull Soc Zool Fr 108:289–301
199. Merlin JC, Delé-Dubois ML (1986) Comp Biochem Physiol B Biochem Mol Biol 84B:97–103
200. Merlin JC, Delé-Dubois ML (1985) In: Alix AJP, Bernard L, Manfait M (eds) Spectrosc Biol Mol, Proc Eur Conf, 1st, Wiley, pp 357–359
201. Karampelas S, Fritsch E, Rondeau B, Andouche A, Métivier B (2009) Gems Gemol 45:48–52
202. Fan L, Yang M (2008) J China Univ Geosci 19:146–151
203. de Oliveira VE, Castro HV, Edwards HGM, de Oliveira LFC (2010) J Raman Spectrosc. doi:10.1002/jrs.2493
204. Leverette CL, Warren M, Smith MA, Smith GW (2008) Spectrochim Acta A 69:1058–1061
205. Cvejic J, Tambutte S, Lotto S, Mikov M, Slacanin I, Allemand D (2007) Mar Biol 152:855–862